Did major fractures in continental crust control orientation of the Knipovich Ridge–Lena Trough segment of the plate margin?

M. D. MAX AND Y. OHTA

Max, M. D. & Ohta, Y. 1988: Did major fractures in continental crust control orientation of the Knipovich Ridge–Lena Trough segment of the plate margin? *Polar Research 6*, 85–93.

Orientation of the complex Knipovich–Lena spreading/transform system closely follows the secondary shear and extensional orientations that existed within adjacent continental crust prior to rifting. Major dextral faults and shear zones within continental crust appear to have affected both the lower crust and upper mantle during extension and to have caused the localization of the early transform rift system.

M. D. Max, Naval Research Laboratory, Acoustics Division, Washington D.C. 20375, U.S.A.; Y. Ohta, Norsk Polarinstitutt, P.O. Box 158, 1330 Oslo lufthavn, Norway; *June 1987 (revised December 1987).*

One of the more dramatic offsets of a spreading ridge/transform system occurs in the Norwegian–Greenland Sea between the Senja–Greenland and Yermak Fracture Zones. This offset is now comprised of oceanic crust in a rift separating sheared margins (Eldholm et al. 1987). The Knipovich Ridge–Lena Trough (Fig. 1), which forms the offset plate margin between the Mohns and Nansen-Gakkel Ridges (Ohta 1982; Vogt 1986a, b) appears to be composed of segments that depart by up to 20° from a purely orthogonal system. The transforms lie at moderate angles to the continental margins, rather than at higher angles that are more characteristic of the Arctic–Atlantic ridge system. As transforms track the orientation of crustal extension, this ridge segment would appear to be anomalous with respect to rifting because extension is neither parallel to the bounding continental margins nor is it orthogonal.

The offset transforms are seen in bathymetry (Perry et al. 1980) only in the northern end of the Lena–Knipovich ridge, but Vogt (1986a, b) has suggested from magnetic data that transform offsets of the plate margin in the Knipovich Ridge early in the ridge history were more pronounced than they are now. This suggests that the Knipovich Ridge is coalescing into a straighter course with time. Our thesis of extensive early structural control of the plate margin involving an imprint of dextral strain paths onto the early formed oceanic crust is consistent with the concept that as the margin matures, it is less likely to reflect an early structural control; hence the apparent contradiction between the early magnetic striping and the current bathymetry can be resolved. An alternate model for establishment of this N–NNW ridge involving two phases of opening (Eldholm et al. 1987) also shows non-orthogonal ridge/transform orientations in the early opening phase, but introduces significant space problems whose resolution within an orthogonal ridge/transform system is not clear.

In this paper we argue that the large scale geometry of the anomalous transform/rift system suggests a close relationship between transpressional strain in the continental crust prior to rifting and the orientation of the purely 'oceanic' structures.

Major transverse deep structures in Atlantic border continental crust

Kjøde et al. (1978) and Sundvor & Eldholm (1979) show that the Trollfjorden–Komagelv Fault (Fig. 2) and parallel faults in northernmost Norway and faults in the southwestern part of

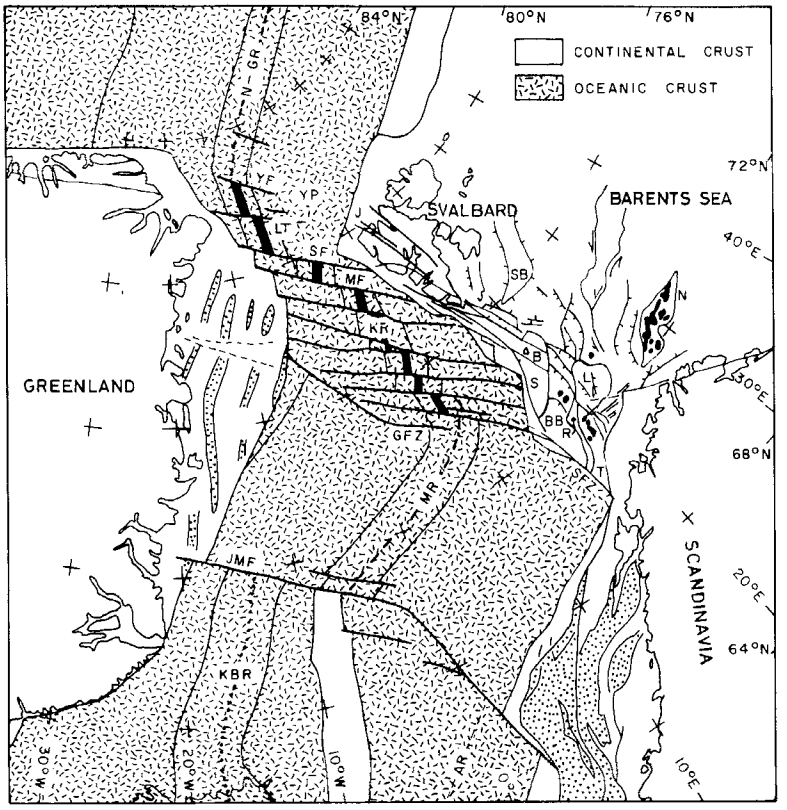

Fig. 1. Present disposition of structural trends in continental and oceanic crust in the North Atlantic region. Transforms near continental crust and the shape of the Greenland margin are speculative, but follow Vogt (1986a, b). Dotted areas are sedimentary basins within the continental crust in the Greenland and Norwegian margin apart from the Barents Sea. Solid, evaporite diapirs at or near the seabed in the southern Barents Sea. AR, Aegir Ridge; B, Bjørnøya; BB, Bjørnøya Basin; GFZ, Greenland Fracture Zone; J, Devonian Boundary Faults; JMF, Jan Mayen Fracture Zone; KBR, Kolbeinsey Ridge; KR, Knipovich Ridge; L, Loppa High; LT, Lena Trough; MF, Molloy Fracture; MR, Mohns Ridge; N, Nordkapp Basin; N-GR, Nansen–Gakkel Ridge; R, Senja Ridge; S, Stappen High; SB, Sentralbanken High; SF, Spitsbergen Fracture; SFZ, Senja Fracture Zone; T, Tromsø Basin; YF, Yermak Fracture; YP, Yermak Plateau. Solid along the Knipovich Ridge is oceanic crust younger than 10 my according to Vogt (1986a, b).

Spitsbergen were wrench faults during the opening of Iapetus in latest Precambrian to Cambrian times. Movement was dextral in relation to Baltica, but sinistral within Svalbard. Harland & Gayer (1972) regarded the Trollfjorden–Komagelv fault as a suture between Baltica and the 'Barents shelf terrane'. To the east (Fig. 4). the fault can be followed across the Arkhangelsk inlet and into Russia (Roberts & Gale 1978) along the southern margin of the Late Precambrian (Baikalian) Kanin-Timian orogenic belt (Siedlecka 1975). The Barents Sea Group, along the northern part of the Varanger peninsula, may have been transported from a position close to present west Spitsbergen. Spitsbergen would have had to have been to the west and north Varanger to the east of Iapetus opening (Kjøde et al. 1978).

A line of faulting within the Caledonian nappes across Finnmark and out onto the Continental shelf (Gee et al. 1985) indicates the course of the Trollfjorden–Komagelv Fault (Fig. 3). Basement faults have apparently propagated upward into the Caledonian thrust sheets. Gudlaugsson et al. (1987) show faults along this line to the middle of the Hammerfest Basin. Faleide et al. (1984) also show WNW faults within the Hammerfest Basin lying along a NW continuation of the Trollfjorden–Komagelv Fault line. These trans-basinal faults were active during the early Tertiary (Riis et al. 1985).

In western Svalbard and the continental margin in the vicinity of Bjørnøya (Bear Island), major Upper Palaeozoic faults, which were repeatedly reactivated in mid-Jurassic and late Cretaceous times, have been followed to the SSE (Rønnevik & Jacobsen 1984). These faults swung to the east in the shelf of late Caledonian times and pass toward the western end of the Trollfjorden–Komagelv Fault zone (Fig. 4). Detailed fault correlation along the strike is difficult, but Rønnevik & Jacobsen (1984) show a persistent NW–SE fault trend. In the late Devonian, faults emanating from southern Svalbard curved to the SE and E through the Stappen High and into the Bjørnøya

Basin. In the mid-Permian, faults emanating from southern Svalbard died out in the Bjørnøya Basin. In the mid-Jurassic, probable sinistral movements along the north side of the Loppa High truncated and deflected NW–SE trending faults in the Bjørnøya Basin. In the top Lower Cretaceous, NW–SE faults existed across the Bjørnøya Basin and east to Bjørnøya. No faults connecting the westward continuation of the Trollfjorden–Komagelv Fault and the SE continuation of the Hornsund Fault system were traced across the Loppa High by Faleide et al. (1984).

An arcuate, major gravity linear can be traced from off the SW coast of Svalbard, where it is about coincident with the continental margin,

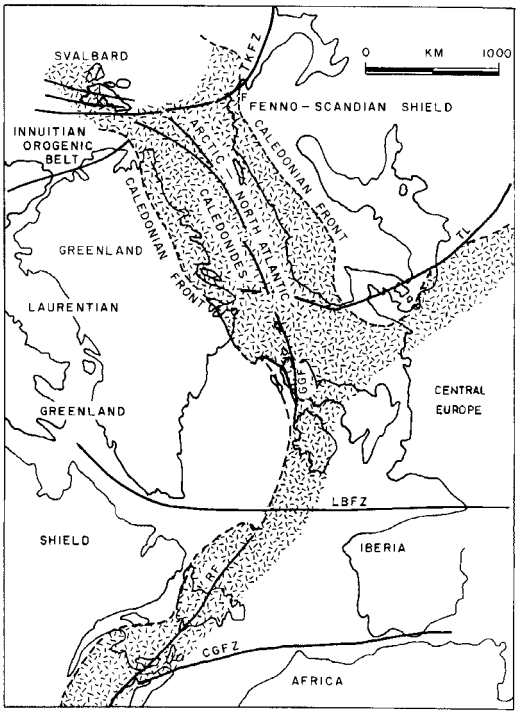

Fig. 2. General geological framework in the supercontinent showing the relationships of major fault lines and the probable positioning of the westward continuation of the Trollfjorden–Komagelv Fault (after Ziegler 1978). F, Finnmark; GGF, Great Glen Fault; RF, Reach Fault. Caledonian orogen in the North Atlantic region patterned; southern Caledonian front not depicted. Note the extent of the transverse fault zones in the North Atlantic region. CGFZ, Cedabucto–Gibraltar Fault Zone; LBFZ, Labrador–Biscay Fault Zone; TKFZ, Trollfjorden–Komagelv Fault Zone; TL, Tornquist Line.

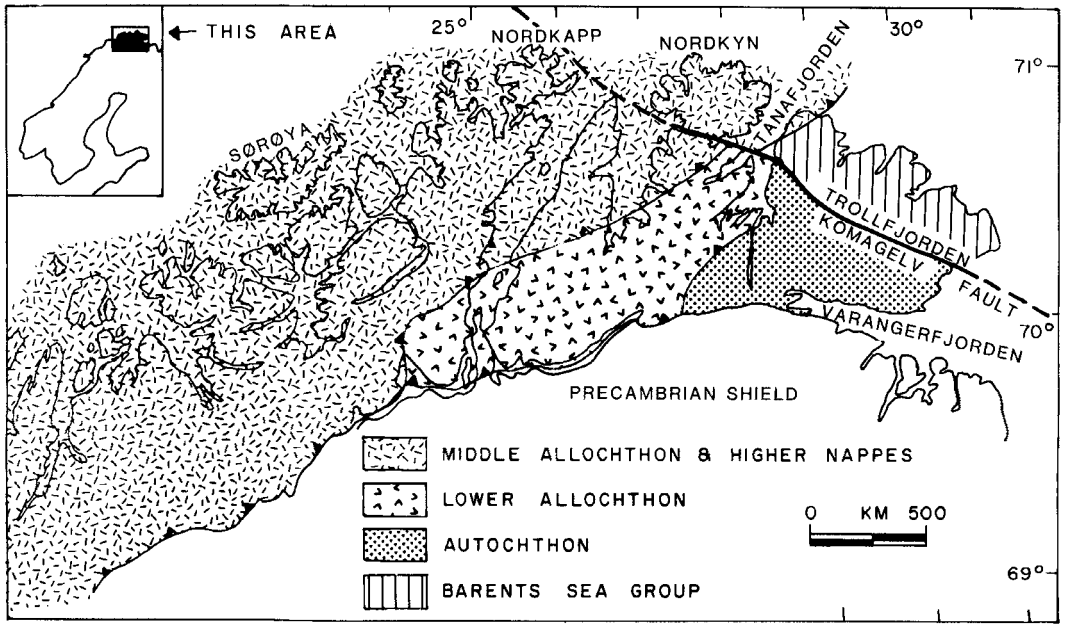

Fig. 3. General geology of the Finnmark area, northernmost Norway showing the high structural level Caledonian Middle Allochthon (nappe front) truncating the westward end of the Trollfjorden–Komagelv Fault and itself being displaced along the fault trace (after Gee et al. 1985). Lower and Middle (and higher) Allochthons are Caledonian in age. Toothed line indicates major thrust fronts. Autochthon includes Precambrian shield and sedimentary cover over shield.

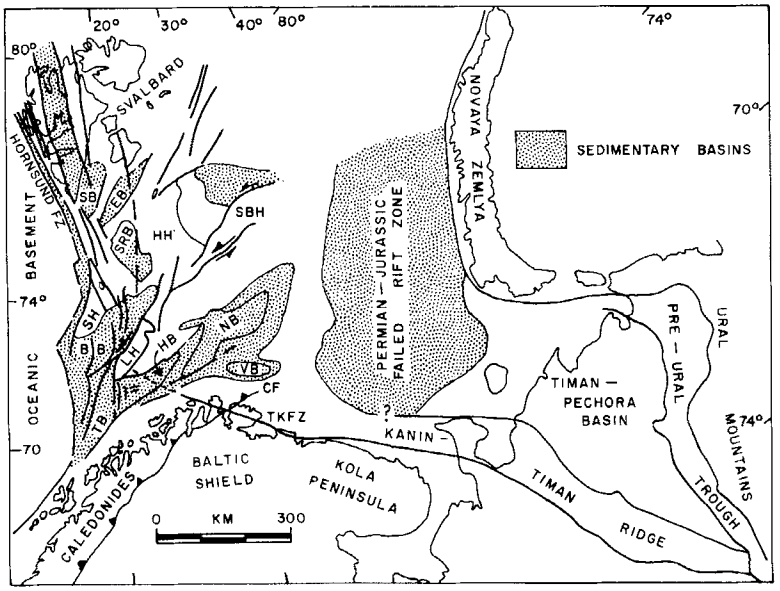

Fig. 4. General geology of the southern and western part of the Barents Sea. Eastward continuation of the Trollfjorden–Komagelv Fault as a structural front carries into the western Ural Mountains forming a feature that is at least 1200 km long. Western continuation is along the complex continental margin and into the nexus of faults that is associated with the Hornsund Fault Zone. CF, Caledonian Front; TKFZ, Trollfjorden–Komagelv Fault Zone. Basins: BB, Bjørnøya Basin; EB, Edgeøya Basin; HB, Hammerfest Basin; NB, Nordkapp Basin; SB, Storfjorden Basin; SRB, Sørkapp Basin; TB, Tromsø Basin; VB, Varanger Basin. Highs: HH, Hopen High; LH, Loppa High; SBH, Sentralbanken High; SH, Stappen High. Arrows on margin of the Sentralbanken High and the Bjørnøya Basin show wrench fault sense. Heavy lines are faults.

southeast toward the Norwegian coast (Riis et al. 1985). It passes as a smooth, undisrupted feature northeast of Bjørnøya through a region of faults stepping down to the NE into the Sørkapp Basin, across the Bjørnøya Basin and through the Loppa High. With a single, small sinistral offset coincident with the margin of Sentralbanken, the linear passes across the Hammerfest Basin coincident with trans-basinal faults, and into the Trollfjorden–Komagelv Fault trace. We regard this gravity linear as marking the subjacent course of a deep, major fault feature.

Faults on a NE–SW trend controlled the elongate boundaries of the Hammerfest, Nordkapp–Bjørnøya and Storfjorden basins and the Stappen, Sentralbanken and Loppa Highs; this trend is one of the three major orientations of basement faults in the northwestern margin of the Barents Shelf (Ohta 1982, 1983). The fault along the SE margin of the Loppa High penetrates the Moho (Gudlaugsson et al. 1987). The Tromsø–Finnmark Fault Zone along NW Norway marks a division between the little-faulted craton of mainland Scandinavia and the Barents Shelf, which suffered extensive faulting. Sinistral faulting on NE–SW trending faults along the Sentralbanken High probably passes along the Loppa High margins. These shears cross our projected westward continuation of the Trollfjorden–Komagelv Fault trend and could explain the local lack of rejuvenation.

Wrench movement of the Hornsund Fault Zone (Sundvor & Eldholm 1979) was driven by dextral transpression (Lepvrier & Geyssant 1984; Vogt 1986a, b); the fault became the plate boundary in anomaly 23 times (52 million years B.P.). The Norway–Svalbard continental margin and its analogue in north Greenland constitute one of the best documented oblique sheared margins in the Arctic–Atlantic rift system (Eldholm et al. 1987). The Hornsund Fault now forms the margin between continental crust of the Svalbard Platform and oceanic crust (e.g. McWhae 1986).

During early Tertiary transpression, northeastward directed thrusting strongly affected the western half of Spitsbergen. These thrusts may now be either truncated at depth within the Hornsund Fault Zone or form a flower structure splay to the steep-dipping Hornsund Fault (Lowell 1972; McWhae 1986). Steep faults in western Svalbard cut shallow faults or thrusts. Lepvrier & Geyssant (1984, 1985) separate strike slip and thrust movement into separate and distinct episodes based on superposition of fault striations. Transient transtensional zones, however, commonly form in transpressional systems and

younger faults commonly cut across major faults of the same strain system (Dickenson 1983).

Basin-dipping, shallow faults commonly root in subjacent extensional faults. Gudlaugsson et al. (1987) show low angle, seaward dipping seismic events in middle and lower crust beneath basins. These may be structural relics of the early Tertiary transpression or they may be new structures, albeit with a partially reactivated origin, that formed during the extensional event leading to rifting.

Gee (1972) suggested that some strike-slip displacements on longitudinal faults in north-central Spitsbergen occurred in Silurian times, prior to or during deposition of Old Red Sandstone. This strike-slip occurred coeval with the culmination of late Silurian–early Devonian/end-Caledonian thrusting in Norway. Ziegler's (1978) reconstruction takes the Great Glen Fault of Britain along the western shelf margin of Norway and *between* Greenland and Svalbard, following the reconstruction of Kjøde et al. (1978) rather than directly into Svalbard (Harland 1978, 1985). Lamar et al. (1986) argue that while some wrench movement may have occurred along the Billefjorden Fault Zone before the mid-Devonian, there could not have been the 200 to 1000 km of late Devonian movement proposed by Harland & Gayer (1972), Harland (1978) and Harland et al. (1984).

Some lower Mesozoic basins in and near Svalbard have faulted margins, which root in deep faults in the metamorphic basement. Formation of these basins dates back to late Silurian–Devonian times with pronounced subsidence during the Carboniferous (Gjelberg & Steel 1979; Steel & Worsley 1984). Basin formation in late Palaeozoic times was probably a response to the dextral E–W or NW–SE shear in the Laurasian supercontinent (Arthaud & Matte 1977; Matte 1986). These basins deepened and filled with Mesozoic and Tertiary strata.

Major continental crust structures and their effect on oceanic lithosphere

Over much of the North Atlantic region, continental crust structural patterns are regarded as having been subsequently expressed in the position and orientation of ridge/transform systems in oceanic crust. Cherkis et al. (1973) related the position of the Gibbs Fracture Zone between Newfoundland and Ireland to major structures in the continental crust. Max & Lefort (1984) also regarded the existence of the Gibbs Fracture Zone and continental fault zones as being genetically related. On a smaller scale, Lefort & Max (1984) and Max (1987) regarded transform faults in the Porcupine Seabight on the Irish shelf as prolongations of steep-dipping dextral faults. Once orthogonal tensional fault/transfer fault systems are established, it would seem that the pattern can be transferred to at least the early oceanic crust within the rift. Transform faults in the Nansen–Gakkel Ridge of the Arctic Ocean line up with some of the north-trending longitudinal faults in northern Svalbard (Fig. 1), and there may be a direct connection between these longitudinal faults and apparent oceanic crust continuations (Ohta 1983).

Major structures of the continental crust are known to penetrate the Moho (Blundell et al. 1985) of the British shelf. Deep-reaching steep longitudinal faults in western Spitsbergen, which control a Devonian and younger graben passing across the western entrance to Isfjorden, show up to 5 km displacement of the Moho (Sellevoll et al. 1982). Deep, low-angle faults south of Edgeøya (Gudlaugsson et al. 1987) imaged on deep seismic lines, suggest Caledonian subduction or compressional fault features.

Transfer of a structural pattern from continental to oceanic crust must involve a relationship between structure and the development of deep seated magmas. Shear would introduce a highly localized ductility contrast in the lithosphere that would most likely affect the underlying mantle by introducing local anisotropy. Steep-dipping faults and shear zones commonly are exploited by igneous intrusion. Water, which is commonly pumped within fault systems, can be expected in deep faults and shear zones; it would have a significant effect on metamorphism, strain rate adaptation, and the development of magma. A line of fault-related magma chambers along an extensional zone, which was localized by downward propagation of crustal structure, could well mature into axial magma chambers in a rift. The early chambers in the zone of mantle upwelling might well continue to be exploited because of the established ductility and other physical–chemical gradients.

Magma chamber alignment adjacent in the continental margin to the northwest of Spitsbergen

appears to have been related to steep-dipping deep faults passing north from the Devonian Graben. These faults in Svalbard are associated with some volcanic activity and a few dykes occur in the Devonian basin. Sellevoll et al. (1982), however, show a c. 3 km transitional zone Moho only under the Central Spitsbergen Tertiary basin that is characteristic of mobilized lower crust or igneous underplating (Hauser et al. 1987). The northern prolongation of this fault, in the middle of the Yermak Plateau, is coincident with a positive magnetic anomaly that suggests submarine volcanics. Amundsen et al. (1987) show several Tertiary–Quaternary volcanic centers aligned along the western margin of the graben. Both upper mantle ultrabasic and lower continental crustal high-temperature granulite xenoliths in the volcanics demonstrate subsided continental crust. The Yermak Plateau itself is considered, on a larger scale, to be a product of a local hot spot (Feden et al. 1979). The Morris–Jessup Plateau to the NE of northern Greenland was once part of the Yermak Plateau, but it has been rifted and separated by spreading of the Nansen–Gakkel Ridge. The position of the early hot spot, high volumes of pre-rift volcanics and a major change in ridge/transform geometry are related to the position of older steep-dipping deep faults that penetrate the Moho in northwestern Svalbard.

In both the Wernicke and delamination models of basin forming related to lower crustal extension (Wernicke & Burchfel 1982), detachment faults or shear surfaces propagate from the surface through the Moho and into the upper mantle (Lister et al. 1986). Magma derived from the mantle is likely to be selectively generated on the upthrown or footwall of the deep-propagating shear. In contrast, the pure-shear symmetrical model that thins the lower crust while suprajacent upper crust responds in a brittle manner and forms sedimentary basins, symmetrically raises the Moho in the region of greatest thinning (McKenzie 1978). In this idealized model of basin formation, the only possibility for a fault system seen on the surface to propagate through the Moho is by rejuvenation of steep shear zones.

Detachment faults form in rifted continental crust at passive margins. Characteristically, steep-dipping transfer faults lie about normal to the surface trace of the detachment faults, in which they root (Gibbs 1984), and they commonly form in the half-graben complex overlying detachment faults (Lister et al. 1986). These transfer faults are shear surfaces that develop orthogonally and allow adjacent half-graben segments to develop independently. They perform a similar function to transform faults in oceanic crust in separating crustal segments. In a newly forming passive margin, both steep-dipping shears that are longitudinal to rifts and new transfer faults that are orthogonal to the rift trend, offer a path of propagation into oceanic lithosphere. If a strongly defined chain of early magma chambers were established under structural control, its presence might well fix transform/ridge orientations of a new plate margin.

Strain and the structural pattern in the continental crust

Dextral strain will set up a regular pattern of secondary shear and tensional structures related to the orientation and degree of compression within the primary major shearing path. Fig. 5a shows the orientation structures with increasing compressional strain. As the strain increases, the secondary shear elements rotate toward the primary plane. In extreme cases, for instance in mylonites, primary, synthetic and antithetic shears all lie statistically in the same plane with divergence only near strain inhomogeneities. The plane of extension coincidentally rotates toward an orthogonal position with respect to the primary major shears (Fig. 5a, state 3). In extreme cases rotation may be greater than 90°.

Long axes of the sedimentary basins in the northern part of the North Sea, the west Norwegian–Greenland Sea and the western part of the Barents Sea continental shelves have a common N–S trend. This is parallel to basins in the Irish Shelf that formed in response to a dextral wrench on northwest trending shear zones (Lefort & Max 1984). A subsequent extensional event associated with the development of the North Atlantic northward from the Labrador–Biscay Fault Zone formed rifts that lay along a more clockwise trend, and cross-cuts this older extensional basin trend (Fig. 5b).

Widespread late and post-Hercynian dextral movement along major faults that were transverse to the proto-north Atlantic took place from the southern Appalachians to the Finnmark–Svalbard region (Ziegler 1978). These major dextral shears formed during Hercynian tectonism and reac-

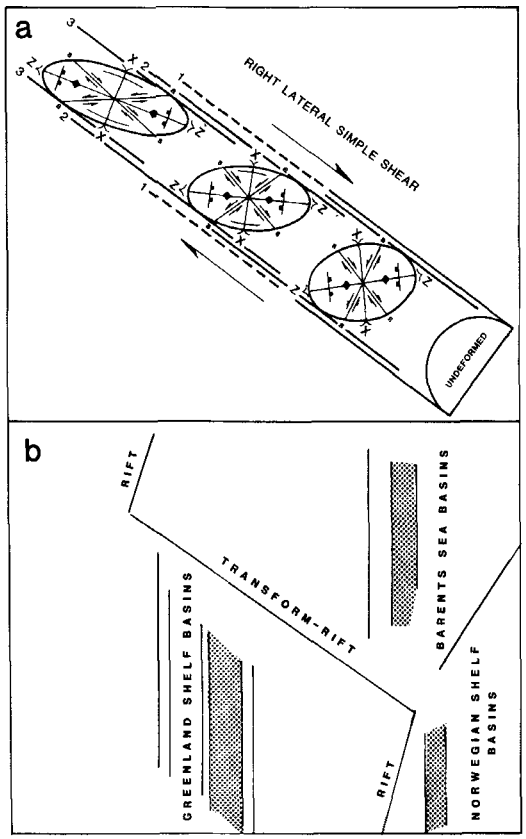

Fig. 5. a. Relationship of transpressional dextral shearing strain. 1–3, deformation and rotation of the deformational ellipsoid with increasing strain. The consequent rotation and change are in angular relationships between the secondary and the primary shear paths. Primary shear oriented to rough parallelism with the present Hornsund FZ (north vertical). X, axis of principal compressive strain; Z, axis of minimum compression (ZY is the plane of flattening); s, synthetic shear; a, antithetic shear.

b. Disposition of the older sedimentary basins (patterned) after Vogt (1986a, b) and the generalized line of the Tertiary rift and wrench fault system (heavy line).

tivation of already existing major structural breaks in the earth's crust (Matte 1986). Although the early extensional and the rifting events might have been formed under other influences, their geometry and timing suggest that establishment of the rifting trend could have been a natural consequence of increased transpressional dextral strain within the northwest trending dextral fault system. With increasing compression across the primary shear trend, the axial plane of the direction of extension within this shear couple would have moved to a more clockwise position (Fig. 5a).

Movement along the Trollfjorden–Komagelv/Hornsund Fault Zone (HTKFZ) compensated spreading to the south of the Greenland–Senja FZ. The nexus of faults that parallels the SW coast of Spitsbergen roughly parallels the continental margin. The Tromsø and Hammerfest Basins, that lie on the continuation of the HTKFZ, appear to form a separate structural area. These basins are more narrow and offset from their eastern prolongations. The northern terminations of the Bjørnøya, Stappen and Loppa Highs (Fig. 1) are also parallel, and close to, this line. The breadth of the shear zone in the continental crust may be picked out by the location of the profusion of

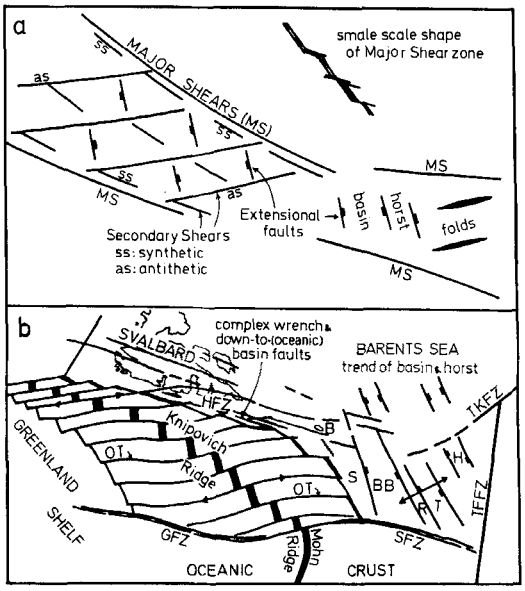

Fig. 6. a. Strain paths in the proto-rift continental crust in high compressional strain transpression; AS, antithetic shear path; MS, major shear path; SS, synthetic shear path. Pattern of major and secondary shears and faults would be repeated at a variety of scales.

b. Diagrammatic relationships between the orientation of the Knipovich Ridge system and the Barents Sea continental margin. Transforms offset spreading ridge creating oceanic crust. Note that the direction of offset on the transforms coincides with the sense of movement on the antithetic strain path related to the sheared continental margins. The surface trace of an individual fault in a closely related set (HFZ) should not be expected to have acted as *the* major shear throughout the history of shearing and basin formation. GFZ, Greenland Fault Zone; HFZ, Hornsund Fault Zone; OT, oceanic transform; SFZ, Senja Fault Zone; R, Senja Ridge; TKFZ, Trollfjorden–Komagelv Fault Zone; TFFZ, Tromsø–Finnmark Fault Zone; arrows indicate the direction of extension. The Hornsund Fault Zone segment is a complex area of tight, elongate Tertiary sedimentary basins, faults, and basement highs.

transforms that helps to isolate the Knipovich Ridge from the Mohns and Nansen–Gakkel Ridges between the Spitsbergen–Molloy FZ and the Greenland–Senja FZ (Fig. 1). The southern end of the Knipovich Ridge passes into the Senja Fault Zone and the northern margin passes into the northern part of the Hornsund Fault Zone (Fig. 6). Splays of this fault set may penetrate into Spitsbergen as the Kongsfjorden FZ and other faults (Ohta 1982, 1983).

The orientation of the spreading centers of the Knipovich Ridge segment lies about parallel to the antithetic strain path orientation in the pre-rift continental crust (Fig. 5a). The apparent absence of synthetic fault structural elements associated with the continental margins to the Knipovich oceanic segment indicates that compression in the transpressive framework was intense. This indication that compression was important, is also indicated by the antithetic-transform trend, which lies at a relatively low angle to the primary shear along the continental margin. In addition, there is a nearly orthogonal relationship of the axis of the direction of extension and the inherently extensional ridge axis that is at a high angle to the primary major shear (Fig. 6b).

Conclusions

The southern margin to late Precambrian deformation of the Barents Sea Group in North Norway is an important structural line that can be followed along reactivated fault lines westward beneath Caledonian nappes, the North Greenland fold belts (Pearyan and Ellesmerian orogenic zones) and Devonian sedimentary basins on the continental shelf. This line passes into the vicinity of the southeastern end of the Hornsund Fault Zone at a low angle to the south of Bjørnøya. Faults in Svalbard and on the continental shelf that parallel the Hornsund Fault Zone west of Svalbard pass to the east to about the intersection of the Hammerfest Basin and the Barents Sea Group's southern structural front.

The apparent continuity of major, steep-dipping deep faults that may have their origins in the Late Precambrian, in an area that has suffered subsequent extensional tectonics and rifting during formation of the Iapetus and North Atlantic Oceans and mobile belt during Caledonian tectonism, implies that the later events reactivated the older features without annealing or seriously displacing them. Alternatively, annealed areas could have redeveloped these trends by propagation from unannealed regions. As the Caledonian deformation on both the Greenland and Norwegian margins is dominated by thrust tectonics, the zone of deep-seated Caledonian deformation, if any remains, would be confined to a narrow zone in the outer continental shelves. Although faults on a Caledonian trend pass well into the Barents Sea, it is possible that Iapetus also propagated along western Svalbard, utilizing one of the older Late Precambrian faults.

Dextral strain in this region appears to have exploited the orientation of these older structures during the northward migration of the North Atlantic spreading ridge system from the Greenland Sea to the Eurasian basin of the Arctic Ocean. The non-orthogonal relationship of the ridge segments and transforms on the extended Knipovich Ridge probably reflects strain vectors inherited from Tertiary and older rifting of continental crust.

Acknowledgements. – Many thanks to P. Vogt for discussions on the geology and geophysics of this area and for access to his collection of data.

References

Amundsen, H. E. F., Griffin, W. L., O'Reilly, S. Y. 1987: The lower crust and upper mantle beneath northwestern Spitsbergen: evidence from xenoliths and geophysics. *Tectonophysics 139*, 169–185.

Arthaud, F. & Matte, P. 1977: Late Paleozoic strike-slip faulting in southern Europe and northern Africa: Result of a right-lateral shear zone between the Appalachians and the Urals. *Geological Society of America Bulletin 88*, 1305–1320.

Blundell, D. J., Hurich, C. A. & Smithson, S. B. 1985: A model for the MOIST seismic reflection profile, N Scotland. *Geological Society of London Journal 142*, 245–258.

Cherkis, N. Z., Fleming, H. S. & Massingill, J. V. 1973: Is the Gibbs Fracture Zone a westward projection of the Hercynian Front into North America? *Nature 245*, 113–115.

Dickenson, W. R. 1983: Cretaceous sinistral strike slip along Nacimiento Fault in coastal California. *American Association of Petroleum Geologists Bulletin 67*, 624–645.

Eldholm, O., Faleide, J. I. & Myhre, A. M. 1987: Continent-ocean transition at the western Barents Sea/Svalbard continental margin. *Geology 15*, 1118–1122.

Faleide, J. I., Gudlaugsson, S. T. & Jacquart, G. 1984: Evolution of the western Barents Sea. *Marine and Petroleum Geology 1*, 123–150.

Feden, R. H., Vogt, P. R. & Fleming, H. S. 1979: Magnetic and bathymetric evidence for the 'Yermak Hot Spot' northwest of Svalbard in the Arctic Basin. *Earth and Planetary Science Letters 44*, 18–38.

Gee, D. G. 1972: Late Caledonian (Haakonian) movements in northern Spitsbergen. *Norsk Polarinstitutt Årbok 1970*, 92–101.

Gee, D. G., Kumpulainen, R., Roberts, D., Stephens, M. B., Thon, A. & Zachrisson, E. 1985: Scandinavian Caledonides Tectonostratographic Map (1:2,000,000). In Gee, D. G. & Sturt, B. A. (eds.): *The Caledonide Orogen – Scandinavia and Related Areas*. John Wiley & Sons, London.

Gibbs, A. D. 1984: Structural evolution of extensional basin margins. *Geological Society of London Journal 141*, 609–620.

Gjelberg, J. & Steel, R. 1979: Middle Caboniferous sedimentation in relation to tectonic, climatic and sea level changes on Bjørnøya and Spitsbergen. *North Sea Symposium, Tromsø. NSS/27*.

Gudlaugsson, S. T., Faleide, J. I., Fanavoll, S. & Johansen, B. 1987: Deep seismic reflection profiles across the western Barents Sea. *Geophysical Journal of the Royal Astronomical Society. Special Issue of Deep Seismics*, 273–278.

Harland, W. B. 1978: The Caledonides of Svalbard. Pp. 3–11 in *Caledonian–Appalachian Orogen of the North Atlantic Region. Geological Survey of Canada Paper 78–13*.

Harland, W. B. 1985: Caledonide Svalbard. Pp. 999–1016 in Gee, D. G. & Sturt, B. A. (eds.): *The Caledonide Orogen – Scandinavia and related areas*. John Wiley & Sons, London.

Harland, W. B., Cutbill, J. C., Friend, P. F., Gobbett, D. J., Holliday, D. W., Maton, P. I., Parker, J. R. & Wallis, R. H. 1984: The Billefjorden Fault Zone, Spitsbergen. *Norsk Polarinst. Skr. 161*. 72 pp.

Harland, W. B. & Gayer, R. A. 1972: The Arctic Caledonides and earlier oceans. *Geological Magazine 109*, 289–314.

Hauser, E., Potter, C., Hauge, T., Burgess, S., Burtch, S., Mutschler, J., Allmendinger, R., Brown, L., Kaufman, S. & Oliver, J. 1987: Crustal structure of eastern Nevada from COCORP deep seismic reflection data. *Geological Society of America Bulletin 99*, 833–844.

Kjøde, J., Storetvedt, K. M., Roberts, D. & Gidskehaug, A. 1978: Palaeomagnetic evidence for large-scale dextral movement along the Trollfjord–Komagelv Fault, Finnmark, North Norway. *Physics of the Earth and Planetary Interiors 16*, 132–144.

Lamar, D. L., Reed, W. E. & Douglass, D. N. 1986: Billefjorden Fault zone, Spitsbergen: Is it part of a major Late Devonian transform? *Geological Society of America Bulletin 97*, 1083–1088.

Lefort, J. P. & Max, M. D. 1984: Development of the Porcupine Seabight: use of magnetic data to show the direct relationship between early oceanic and continental structures. *Geological Society of London Journal 141*, 663–674.

Lepvrier, C. & Geyssant, J. 1984: Tectonique cassant et champs de contrainte tertiaires de long de la marge en coulissement du Spitsberg: Corrélations avec les méchanismes d'ouverture de la mer de Norvège–Groënland. *Ann. Soc. Géol. Nord III*, 333–344.

Lepvrier, C. & Geyssant, J. 1985: L'évolution structurale de la marge occidentale du Spitsberg: coulissement et rifting tertiaires. *Bulletin Société géologique de France 87(1)*, 115–125.

Lister, G. S., Etheridge, M. A. & Symonds, P. A. 1986: Detachment faulting and the evolution of passive continental margins. *Geology 14*, 246–250.

Lowell, J. D. 1972: Spitsbergen Tertiary Orogenic Belt and the Spitsbergen Fracture Zone. *Geological Society of America Bulletin 83*, 3091–3102.

Matte, P. 1986: La chaine varisque parmi les chaines paléozoïques péri atlantiques, modèle d'évolution et position des grands blocs continentaux au Permo-Carbonifére. *Bulletin Société géologique de France 8*, 9–24.

Max, M. D. 1987: The three phase development of the Porcupine Seabight Basin formation and the sedimentary pattern. *Journal of Petroleum Geology 10*, 59–72.

Max, M. D. & Lefort, J. P. 1984: Does the Variscan front in Ireland follow a dextral shear zone? In Hutton, D. H. W. & Sanderson, D. J. (eds.): *Variscan Tectonics of the North American region. Geological Society of London Special Publication 14*.

McKenzie, D. P. 1978: Some remarks on the development of sedimentary basins. *Earth and Planetary Science Letters 40*, 25–32.

McWhae, J. R. 1986: Tectonic history of northern Alaska, Canadian Arctic and Spitsbergen regions since Early Cretaceous. *American Association of Petroleum Geologists Bulletin 70*, 430–450.

Ohta, Y. 1982: Morpho-tectonic studies around Svalbard and the northernmost Atlantic. Pp. 415–429 in Ashton, F. E. & Balkwill, H. R. (eds.): *Arctic Geology and Geophysics. Canadian Society of Petroleum Geologists Memoir 8*.

Ohta, Y. 1983: Caledonian fractures in Svalbard. Pp. 339–350 in Gabrielsen, R. H., Ramberg, I. B., Roberts, D. & Steinlein, O. A. (eds.): *Proceedings of the 4th International Conference of Basement Tectonics, 1981*.

Perry, R. K., Fleming, H. S., Cherkis, N. Z., Feden, R. H. & Vogt, P. R. 1980: *Bathymetry of the Norwegian–Greenland and western Barents Sea. Naval Research Laboratory, Acoustics Division, 1:2,333,230 map*.

Riis, F., Vollset, J. & Sand, M. 1985: Tectonic development of the Western Margin of the Barents Sea and adjacent areas. *NPD contribution 22*. 14 pp.

Roberts, D. & Gale, G. H. 1978: Caledonian–Appalachian and Iapetus Ocean. Pp. 255–342 in Tarling, D. H. (ed.): *The Evolution of the Earth's Crust*. Academic Press, London.

Rønnevik, H. & Jacobsen, H. P. 1984: Structural highs and basins in the western Barents Sea. Pp. 19–32 in *Petroleum Geology of the North European Margin*. Norwegian Petroleum Society (Graham & Trotman, London).

Sellevoll, M. A., Duda, S., Komber, J., Pajchel, J., Guterch, A. & Perchuc, E. 1982: *Seismic Crustal Studies on Spitsbergen 1978. Seismological Observatory Report, University of Bergen*. 62 pp.

Siedlecka, A. 1975: Late Precambrian stratigraphy and structure of the North–Eastern Margin of the Fennoscandian Shield (East Finnmark – Timian region). *Norges geologiske Undersøkelser 316*, 313–348.

Steel, R. J. & Worsley, D. 1984: Svalbard's post-Caledonian strata – an atlas of sedimentational patterns and palaeogeographic evolution. Pp. 109–135 in Spencer, S. M. et al. (eds.): *Petroleum Geology of the North European Margin*. Norwegian Petroleum Society (Graham & Trotman, London).

Sundvor, E. & Eldholm, O. 1979: The western and northern margin off Svalbard. *Tectonophysics 59*, 239–250.

Vogt, P. R. 1986a: Geophysical and geochemical signatures and plate tectonics. Pp. 413–662 in Hurdle, B. G. (ed.): *The Nordic Seas*. Springer-Verlag, New York.

Vogt, P. R. 1986b: Magnetic anomalies and crustal magnetization. Pp. 229–256, Plate 8B in Vogt, P. R. & Tucholke, B. E. (eds.): *The Geology of North America, Vol. M, The Western North Atlantic Region*. Geological Society of America.

Wernicke, B. & Burchfel, B. C. 1982: Modes of extensional tectonics. *Journal of Structural Geology 4*, 105–115.

Ziegler, P. A. 1978: North-western Europe: tectonics and basin development. *Geologie en Mijnbouw 57*, 589–626.

Expanding spread profile at the northern Jan Mayen Ridge

BÅRD JOHANSEN, OLAV ELDHOLM, MANIK TALWANI, PAUL L. STOFFA AND PETER BUHL

Johansen, B., Eldholm, O., Talwani, M., Stoffa, P. L. & Buhl, P. 1988: Expanding spread profile at the northern Jan Mayen Ridge. *Polar Research 6*, 95–104.

An expanding spread seismic profile at the central northern Jan Mayen Ridge, ESP-5, has yielded a crustal seismic velocity distribution which is similar to observations from the thinned continental crust at the Norwegian continental margin. The profile reveals a post-early Eocene sedimentary sequence, about 1.5 km thick, overlying 1 km of volcanic extrusives and interbedded sediments. Below, there are about 3 km of pre-opening sediments above the seismic basement. The results indicate that the main ridge block is underlain by a thinned crust, possibly only 13.5 km thick. The results are compatible with a continental nature for the main ridge complex.

Bård Johansen, Norwegian Petroleum Directorate, Harstad, Norway, or: *Department of Geology, University of Oslo, Norway; Olav Eldholm, Department of Geology, University of Oslo, Norway; Manik Talwani, Rice University and Houston Area Research Center, Houston, Texas, U.S.A.; Paul L. Stoffa, Institute for Geophysics and Department of Geological Sciences, University of Texas at Austin, U.S.A.; Peter Buhl, Lamont-Doherty Geological Observatory, Palisades, New York, U.S.A.;* *November 1987 (revised February 1988).*

In the fall of 1978 a multichannel seismic program was carried out by the Lamont-Doherty Geological Observatory (L-DGO) and the Universities of Oslo and Bergen. Part of this program included acquisition of 24 fold multichannel seismic profiles (MCS), an Expanding Spread Profile (ESP) and a Constant Offset Profile (COP) to study the crustal nature of the Jan Mayen Ridge (Fig. 1). The acquisition of the geophysical data was performed onboard R/V 'R.D. Conrad' of L-DGO (Leg C21-14), whereas the Norwegian vessel F/F 'H.U. Sverdrup' served as a shooting ship during the ESP and COP experiments.

The submarine Jan Mayen Ridge, which constitutes the border between the deep Norway Basin and the Iceland Plateau, is bounded to the north by the West Jan Mayen Fracture Zone and the island of Jan Mayen. The ridge forms a single block-like feature north of 68.6°N, changing into a series of northeast trending smaller ridges plunging southwards to about 67.3°N where there is no bathymetric expression of the ridge. The main ridge block is separated from the South Jan Mayen Ridge by the linear Jan Mayen Trough (Fig. 1).

The structure, composition and evolution of the ridge have been addressed in a number of studies based on both geophysical data and DSDP drilling. The results have been summarized by Myhre et al. (1984). In particular, data from MCS surveys have much improved the understanding of the geologic setting (Gairaud et al. 1978; Eggen 1984; Johansen 1988; Skogseid & Eldholm 1987; Gudlaugsson et al. 1988), although the deep ridge structure is still poorly understood. It is generally believed that the Jan Mayen Ridge represents a fragment of the East Greenland continental margin, finally separated prior to anomaly 6 time (20 Ma) (Talwani & Eldholm 1977; Nunns 1983). We note, however, that no pre-opening rocks have yet been collected from the ridge and that the boundaries of the microcontinent are largely uncertain. The ridge has a clear gravity signature (Fig. 2) which is compatible with a continental nature (Grønlie & Talwani 1982).

In this study, we present the analysis of the L-DGO expanding spread profile (ESP-5, Fig. 1) and discuss the results in terms of the crustal properties of the main northern ridge block. We have also included new bathymetric and free-air gravity anomaly maps (Figs. 1 and 2) compiled by integrating the 1978 data with the existing database (Johansen 1988). Interpretation of the L-DGO MCS profiles has been presented by Johansen (1988) and Skogseid & Eldholm (1987). The geophysical data acquired by the

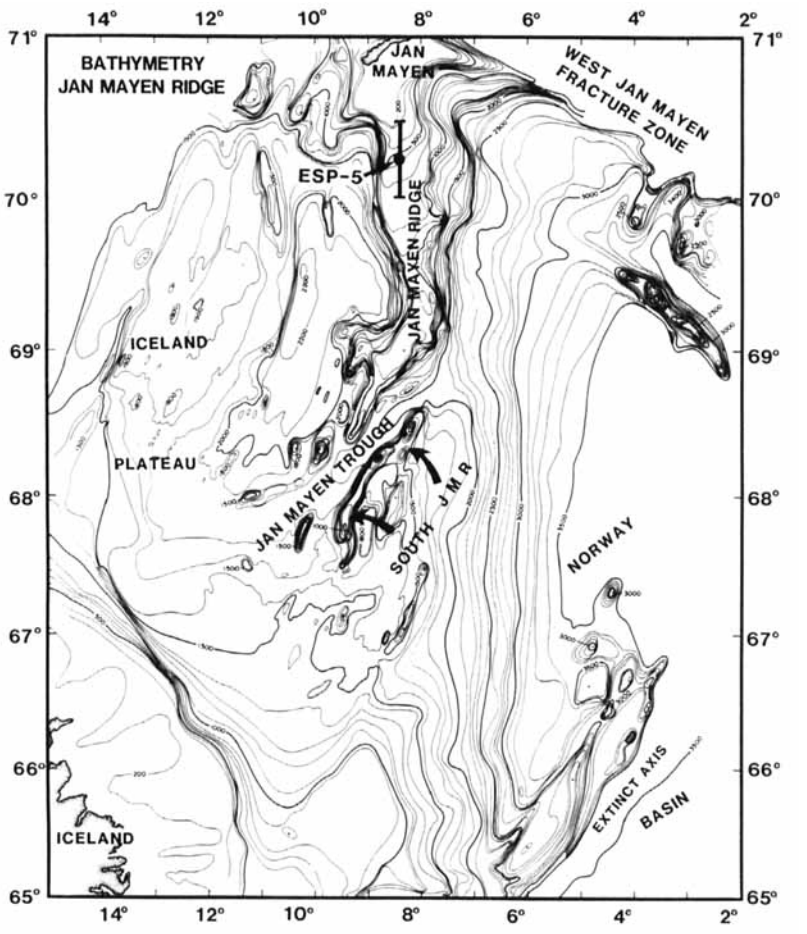

Fig. 1. Bathymetry, in corrected meters, of the Jan Mayen Ridge and environs. Contour interval 100 m. The map is constructed from a database described by Johansen (1988). ESP-5 is located at the central part of the northern Jan Mayen Ridge. The position of the common midpoint is: 70°14′N, 8°20′W, and the northern and southern end points are located at 70°29′N, 8°21′W and 69°19′N, 8°19′W, respectively.

accompanying Norwegian vessel have been presented by Myhre et al. (1984).

Expanding spread profile

An ESP experiment is a spatially localized, wide-angle reflection/refraction profile using two ships, a multichannel receiver array and an accurate ranging system. The experiment is particularly valuable because of the fidelity with which the data are recorded and the multiplicity of coverage provided by the array. As it yields good quality time, amplitude and range information, we are able to perform detailed inversion and modelling (Stoffa & Buhl 1979). This task is carried out by transforming the observational data from the distance-travel time (x-t) plane into the plane of intercept time and horizontal ray parameter (tau-p). Subsequently, the data are inverted, yielding the vertical variation in velocity as a function of depth (Stoffa & Buhl 1979; Diebold & Stoffa 1981). Profile ESP-5 has been reduced and inverted in this manner, although some small modifications described below have been introduced to better resolve the crustal nature of this relatively shallow ridge.

Field procedure

During the acquisition of ESP-5, the shooting ship and the recording ship steamed apart on a predetermined course at a speed of about 9 km/h (5 knots) (Fig. 3). 3.5 kg explosive charges were detonated every minute along the first 5 km of the profile. Then the charge size and detonation interval increased with the range, and at the far distances 50 kg charges were dropped every

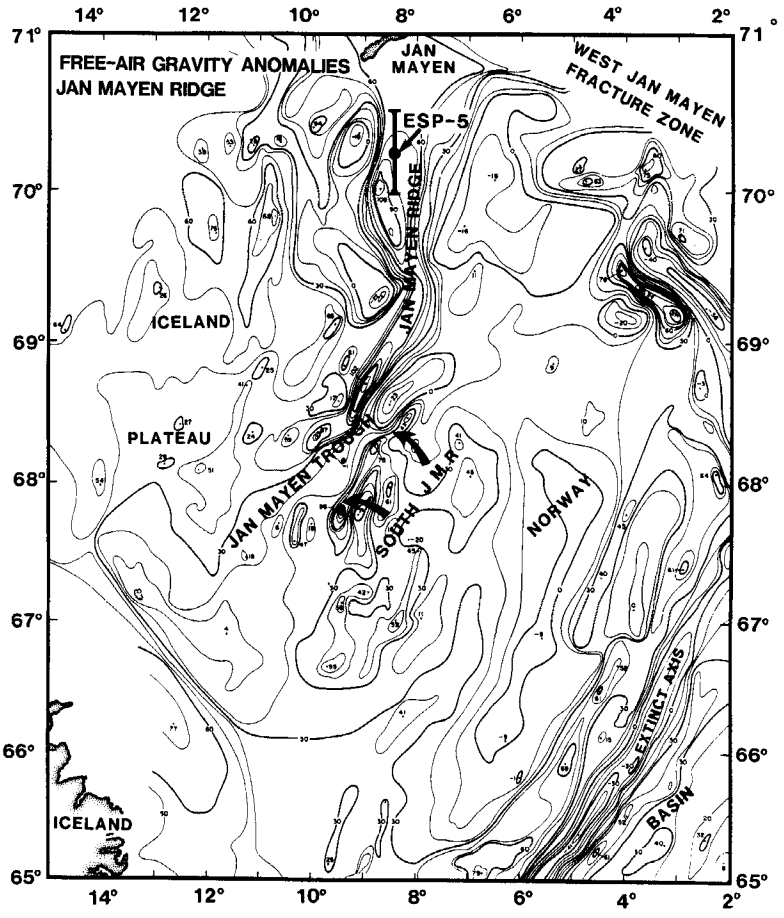

Fig. 2. Free-air gravity anomaly map of the Jan Mayen Ridge and environs. Contour interval 10 mGal. Constructed from a data base described by Johansen (1988).

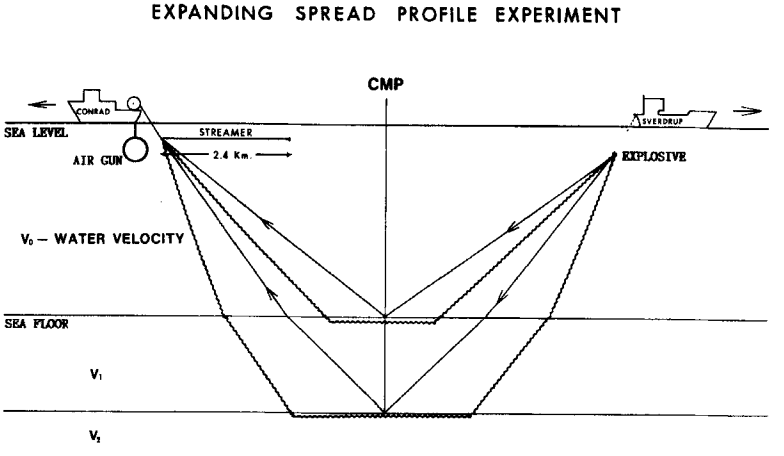

Fig. 3. Sketch of the Jan Mayen Ridge two-ship Expanding Spread field experiment. CMP refers to the common midpoint.

4 min. The firing schedule was determined to yield a continuous subsurface coverage along the entire profile. The total length of ESP-5 is about 50 km, extending 25 km on either side of the common midpoint (Fig. 4).

The recording length was 39 s, initially allowing 21 s to record a normal CDP profile by firing the 'R.D. Conrad' airguns between the charges. This interrupted recording pattern resulted, of course, in varying and often low fold CDP gatherers. The fold, however, improved with increasing ESP range when the explosive charges were detonated less frequently. Velocity analyses were also performed on the CDP data which were gathered in 50 m bin separation and stacked with lower folds to obtain continuous subsurface coverage.

The principal advantage of an ESP experiment is dependent on accurate recordings of the travel times, shot instant and signal amplitude with the continuously increasing distance between the vessels. Every shot was recorded with true amplitude on the field tapes. Moreover, by using a 24-traces with known (100 m) spacing, we could eliminate static timing errors in travel times from subsequent velocity determinations by adjusting each shot as needed, using the arrival of the direct water wave. The distance was recorded by a Raydist range determination system allowing an accuracy of 5 m (Stoffa & Buhl 1979).

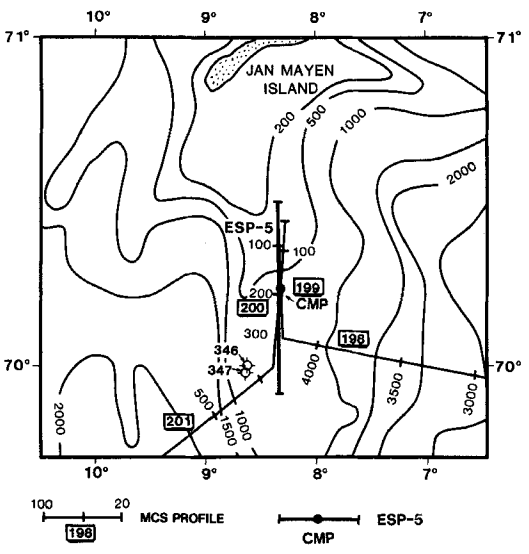

Fig. 4. Location map of ESP-5, adjacent MCS profiles recorded by R/V 'R.D. Conrad' in 1978 and DSDP drillsites 346 and 347.

Data analysis

After demultiplexing and reformating the field tapes, the explosive and airgun shots are separated. Then, we largely follow the procedure of Stoffa & Buhl (1979). First, the data are organized on a shot-trace distance basis, that is, plotting the traces as a function of distance between the shot and receiver (Fig. 5). This makes it possible to perform a velocity scan over more than the 2.4 km streamerlength, detecting weak, deep arrivals. Similarly, we can shorten the aperture of the scan for arrivals at short distances where the signal-to-noise ratio is good and hyperbolically reflected arrivals dominate.

The data in the shot-trace distance (x-t) plane have been transformed into the tau-p plane by a primarily automatic computer procedure, using coherency statistics to define the amount of trace-to-trace coherence for a given phase velocity over a specified aperture (Stoffa & Buhl 1979; Stoffa et al. 1981). For the entire record length, all realistic velocities are scanned (slant-stacked) and the maximum coherence determined over the aperture by the amplitude independent semblance coefficient. The aperture is moved along the profile and the procedure repeated, finally resulting in a plot showing the coherency of all the slant stacks performed. This representation, which contains the original reflection/refraction information, can in a simple manner be inverted to a velocity-depth curve by the tau-sum method (Diebold & Stoffa 1981).

Originally, this procedure was developed for deep water profiles (depths greater than about 3 km) where even weak coherent signals may be isolated. At shallow and intermediate waters, such as the Jan Mayen Ridge, we found this approach unsatisfactory because strong multiple signals in the water column partly suppress the weaker arrivals from deeper in the section. To avoid part of the multiple energy, we designed a window in the x-t plane, accepting data within 1 s of the first arrivals. Only the remaining data were transformed into the tau-p plane.

Fig. 5 shows ESP-5 plotted on a shot-trace distance basis in the x-t domain. Here, the zero distance refers to the common midpoint (CMP), which is the actual reference location for the velocity-depth curve. After performing velocity scans over linearly increasing overlapping apertures (1.8–10 km), the data are plotted in the domain of intercept-time and ray parameter.

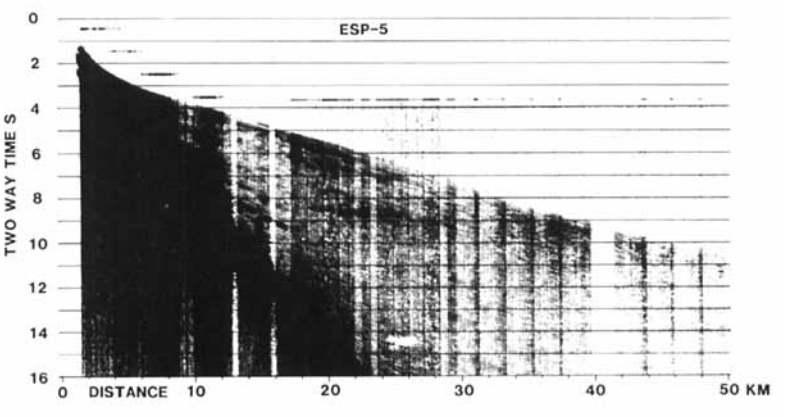

Fig. 5. The ESP-5 observational data arranged in a range sequential order in the x-t domain.

Maximum amplitudes were picked automatically by the computer for each ray parameter, and later edited by hand to define the primary tau-p curve used for the inversion (Fig. 6). Prior to this step, each trace is Hilbert transformed and the envelope of the resulting complex trace is computed to facilitate the maximum amplitude selection. Fig. 6 also includes points representing 84% of the maximum amplitude to obtain one standard deviation error in the intercept-time. The tau-sum determined velocity-two-way travel time and velocity-depth curves are shown in Fig. 7. This solution is accomplished by iterating the travel time equation using intercept-times, slownesses and confidence bounds from Fig. 6 as described by Stoffa et al. (1981). Finally, the solution is superimposed on MCS profile 199 (Fig. 4) derived from the airgun shots recorded between the explosive charges (Fig. 8).

Crustal structure of the main ridge block

Two regional reflectors have been recognized in seismic profiles at the northern ridge segment. The uppermost, JA, which partly has an erosional character is of Upper Oligocene age (Talwani, Udintsev et al. 1976), whereas Gairaud et al. (1978) related the lower, JO, to a rift unconformity associated with the initial opening of the Norwegian-Greenland Sea. Reflector JO onlaps a strongly faulted structural high forming the westernmost part of the ridge. Structuring, including seaward dipping reflectors, has been observed beneath JO (Skogseid & Eldholm 1987; Gudlaugsson et al. 1988) and the structural setting is shown in Fig. 9. Skogseid & Eldholm (1987) have mapped a region of seaward dipping reflectors consisting of a typical inner part (zone IIIA, Fig.

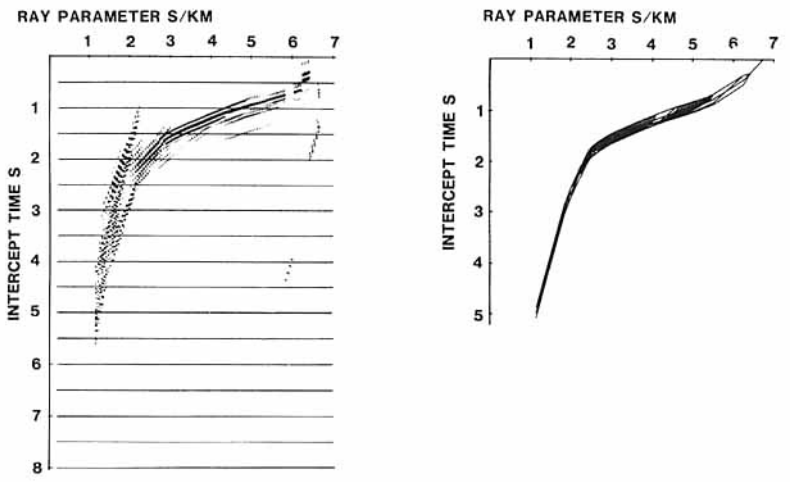

Fig. 6. Left: The x-t data in Fig. 5 transformed into the tau-p plane. Right: The primary tau-p curve including 84% confidence bounds plotted as an envelope around the primary curve.

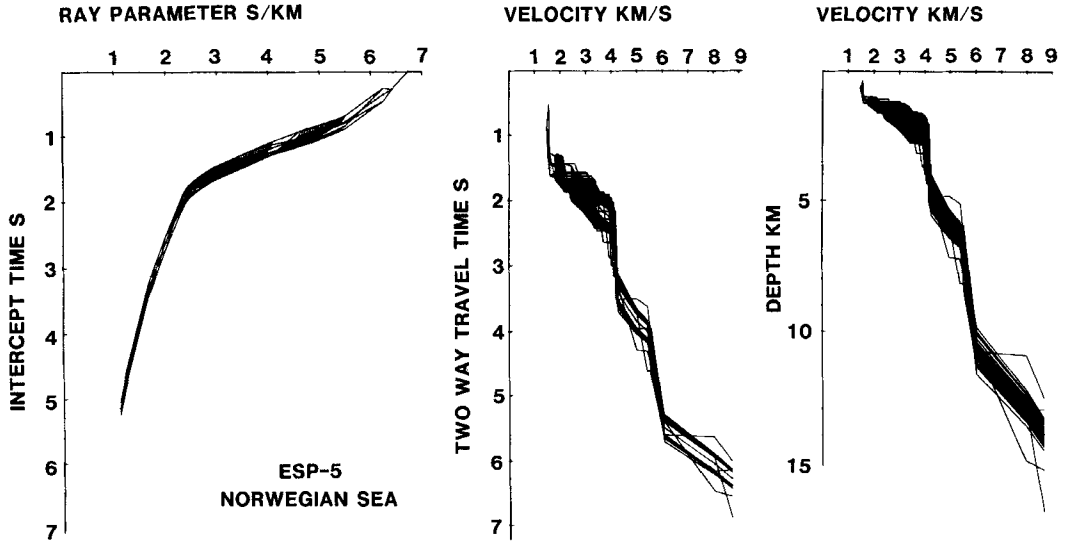

Fig. 7. Tau-sum inversion of the primary tau-p path for ESP-5 (left). Velocity-Twt curve (center) and velocity-depth curve (right). Both include depth ranges defined by a one standard deviation uncertainty in the intercept-time.

9) and a more poorly developed outer part (IIIB). They also proposed that JO is the equivalent to the early Eocene flows at the conjugate Norwegian margin. Fig. 9 shows that ESP-5 is located close to the pinch-out of the dipping wedge, between the western fault zone and the suggested location of the continent-ocean boundary.

The velocity-depth function in Figs. 6 and 7 reveals that only minor smoothing yields a layered model in which the velocity increases linearly with depth within each layer, whereas distinct changes in velocity gradient exist between the layers. The main gradient changes occur at velocities of 1.7, 3.7, 4.0, 4.1, 5.2 and 6.1 km/s, yielding individual layer velocity gradients of 0.50, 1.69, 0.27, 0.08, 0.69, 0.18, and 0.91 s^{-1}, respectively (Fig. 10). For simplicity, we accept this curve as representative of ESP-5 and apply it in the subsequent discussion.

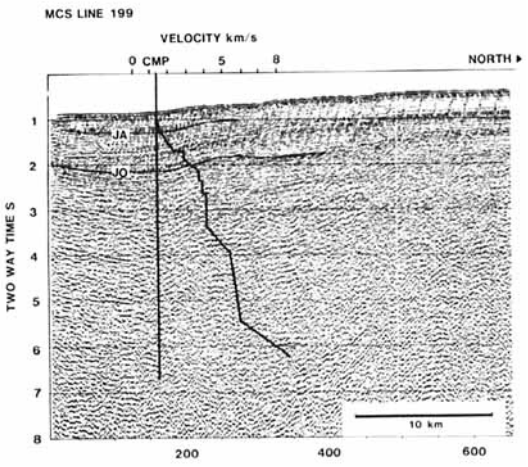

Fig. 8. The velocity-Twt solution for ESP-5 plotted onto MCS profile 199 recorded simultaneously with ESP-5. Location in Fig. 4. JA and JO indicate reflectors described in the text.

It is evident from Fig. 8 that the multiples have not been satisfactorily removed from profile 199. However, using ties to adjacent lines we have identified a distinctive JA horizon at about 1.20 s and a less clear JO reflector at about 2.15 s. These reflectors correlate with the changes in velocity gradients at the 1.7 and 3.7 km/s velocities, respectively. No deeper reflectors have been recognized in profile 199. The poor seismic continuity at and below JO is partly caused by a low signal-to-noise ratio in the vertical incidence record. This is to be expected as profile 199 only yields 6-fold coverage, being recorded simultaneously with ESP-5. Nevertheless, the record gives the general impression of layer shallowing towards the north.

There is good agreement between ESP-5 and the adjacent sonobuoy profiles (Myhre et al. 1984) for the sequences above JO, although the sonobuoys indicate higher velocities at shallower levels

below JO than ESP-5. These differences probably reflect the highly structured relief below JO at the central and western ridge block, documented by Skogseid & Eldholm (1987) and Gudlaugsson et al. (1988).

Assuming that the velocity gradient change at 6.2 km depth represents a sub-JO acoustic basement surface, an early Tertiary age for reflector JO implies an about 4.5 km thick sequence of pre-Eocene sediments below JO. The basement velocity increases gently, reaching 6.1 km/s at a depth of about 11.2 km. At this level there is a more rapid increase in the velocity and an 8.2 km/s 'mantle' velocity is reached at about 13.5 km. We are somewhat uncertain about the steep, 0.91 s^{-1} velocity gradient in the deepest layer. It has been noted (Eldholm & Mutter 1986) that it is often difficult to distinguish between the pre- and post-critical parts of the deepest quarter-ellipse in the tau-p domain. This might also be the case for ESP-5 (Fig. 6). If pre-critical arrivals are inverted a greatly increased velocity gradient can be expected at the deepest part of the velocity-depth curve. On the other hand, our result is supported by OBS-measurements by Weigel & Gebhardt (1986). At about 70°50'N they report an apparent velocity of 8.5 km/s at a depth of about 13 km beneath the central ridge, whereas a crustal thickening is indicated beneath the dipping reflector sequence at the eastern ridge flank.

In terms of the crustal nature in the vicinity of ESP-5 we shall consider two alternative geological models. In one model, we assume that the rocks below JO form a volcanic edifice, e.g. similar to an oceanic plateau or a submarine ridge with an abnormally thick oceanic crust. In the other model, a microcontinent, JO is underlain by continental rocks that originally were part of a passive continental margin that had undergone stretching and thinning prior to the formation of oceanic crust. Examples of these models incorporating the velocities measured in ESP-5 are shown in Fig. 10. The expanded oceanic crustal model is based on the suggestion of Mutter et al. (1984) that the Outer Vøring Plateau represents this type of crust being composed of an expanded layer 2 over an approximately normal oceanic layer 3. The microcontinent model includes an early Cenozoic extrusive sequence to conform with the geological position of ESP-5 (Fig. 9). Thus, both models take into account the suggested genetic similarity between JO and reflector EE at the Vøring Plateau (Skogseid & Eldholm 1987), as well as the observation that the dipping reflectors at the Vøring Plateau consist of early Eocene tholeiitic extrusives and intercalated sediments. Finally, we note that the seismic velocity below reflector JO, 3.7–4.0 km/s, is indeed similar to the one in the drilled dipping sequence at the Vøring Plateau (Eldholm et al. 1987).

Our results show, however, that the velocity-depth relationship in the JA-JO sequence differs from that in Cenozoic units of comparable thickness at the conjugate Norwegian margin where

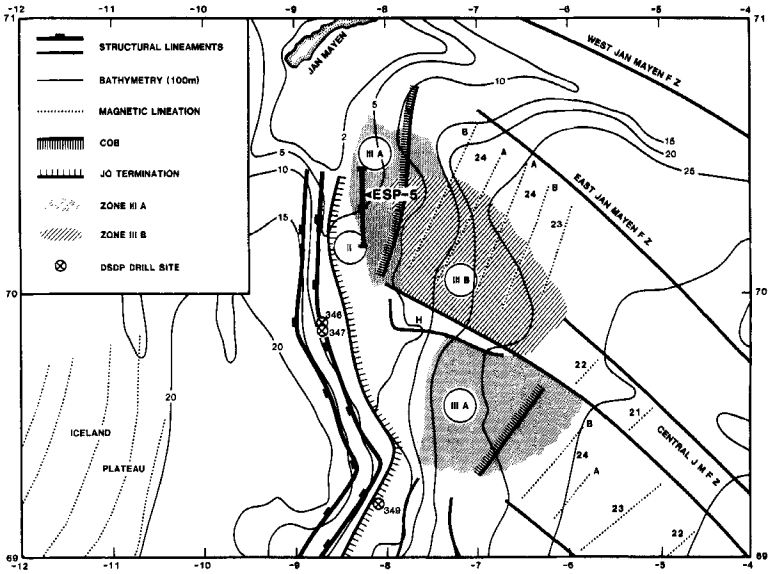

Fig. 9. The location of ESP-5 with respect to main structural features at the level of reflector JO and sea floor spreading magnetic anomalies. COB: continent-ocean boundary. From Skogseid & Eldholm (1987).

velocities in the range of 1.9–2.5 km/s have been observed (Myhre 1984). This could, of course, be an artifact of the poor resolution in the primary tau-p curve at low p values, as discussed by Eldholm & Mutter (1986). On the other hand, the fact that this high sediment velocity is representative for the entire northern ridge led Myhre et al. (1984) to suggest that reflector JO might actually pre-date the early Cenozoic time of opening. This question is still not satisfactorily answered, although Skogseid & Eldholm (1987) present compelling arguments for an early Eocene age of JO. If so, it is probable that the lower JA-JO section comprises a considerable amount of volcanic material associated with the complex evolution of the ridge.

Noting that a pre-Cenozoic age for JO implies a continental fragment below the ridge proper, we now assume an early Eocene age for JO and investigate the crustal implications of ESP-5. In this context, it is considered particularly relevant to compare our results with those from adjacent volcanic oceanic edifices, as well as with data from stretched continental crust that was contiguous with the Jan Mayen Ridge prior to the start of sea floor spreading in the earliest Eocene. Hence, ESP-5 is compared with typical velocity ranges for the crust in eastern Iceland (Mutter et al. 1984) and two ESPs at the conjugate Norwegian margin. ESP-3 (Mutter et al. 1984) is located at the Outer Vøring Plateau Marginal High in a region of transitional crust between the Vøring Plateau Escarpment and anomaly 24B. ESP-2 (Eldholm & Mutter 1986) lies in a region of thinned continental crust in the Vøring Basin just landward of the escarpment. It is evident from Fig. 11 that the ESP-5 sub-JO velocities do not fall within the normal range for Icelandic crust. On the other hand, ESP-5 and ESP-2 exhibit strikingly similar velocity-depth curves. Finally, a comparison of sonobuoy profiles seaward of anomaly 24B at the Outer Vøring Plateau (SBs 273, 331 and 332 of Mutter et al. (1984), see Fig. 11) shows that the main difference with respect to ESP-5 occurs in the sequence just below JO. There is a very gentle velocity gradient at the Jan Mayen Ridge, whereas the velocity indeed increases rapidly with depth at the volcanic marginal high.

The excellent correspondence between ESP-2 and ESP-5 is not surprising in view of the observation that the pre-opening margin sediments off Norway can be separated into regional units by changes in the velocity gradient (Eldholm & Mutter 1986). These changes are associated with velocities of 4.15, 5.0 and 6.2 km/s, values that are indeed close to those measured in ESP-5 (Fig. 10).

Worldwide there is a wide variety in crustal parameters (velocity, thickness) for both microcontinents and oceanic plateaus (Carlson et al. 1980; Forsyth & Mair 1984). The upper crust at the Jan Mayen Ridge appears to be most similar to the Saya de Mahla Bank in the northern Indian Ocean. However, most other microcontinents as well as oceanic plateaus exhibit a greater crustal thickness than the c. 14 km indicated in Fig. 10. For this reason and in view of the possibility of having inverted some pre-critically reflected waves at low p values, we consider the computed

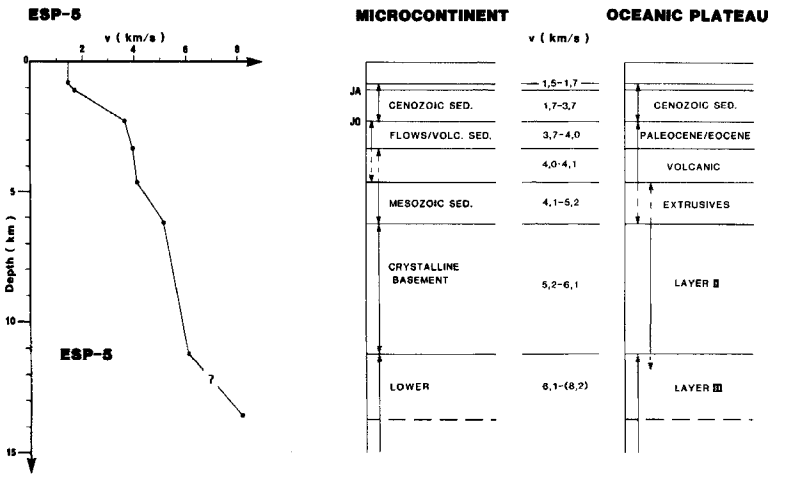

Fig. 10. Simplified velocity-depth curve for ESP-5 (left) and alternative crustal interpretations of the velocity-depth curve (center and right).

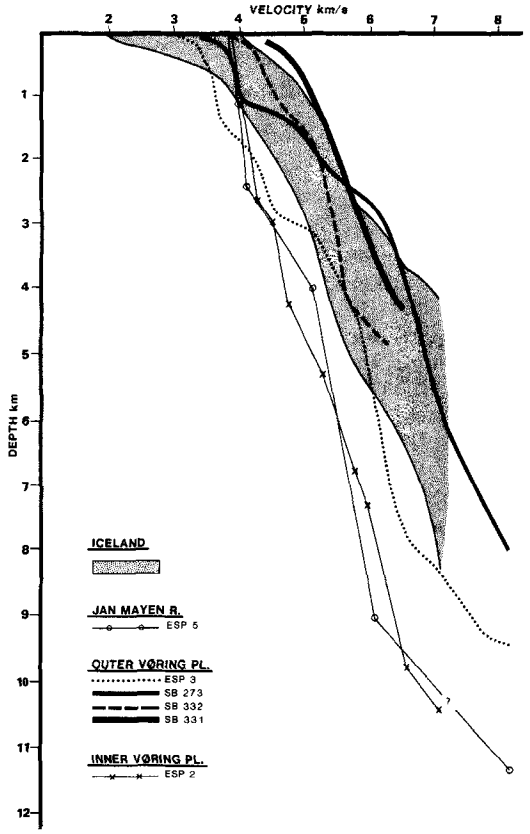

Fig. 11. Comparison of velocity-depth curves from the Jan Mayen Ridge, the Vøring Plateau (the top of the early Eocene volcanics is adjusted to zero depth) and eastern Iceland. ESP-2 is located in the western Vøring Basin (Eldholm & Mutter 1986). ESP-3 lies between the Vøring Plateau Escarpment and the seaward dipping wedge, and the sonobuoys are located seaward of magnetic anomaly 24B at the Vøring Plateau (Mutter et al. 1984). The Icelandic curve is compiled by Mutter et al. (1984).

Moho depth at ESP-5 as a minimum value, though we note that recent ocean bottom seismometer measurements also support a thin crust under the central ridge block (Weigel & Gebhardt 1986).

Conclusion

Separately, the results from ESP-5 do not provide conclusive evidence to determine the crustal nature of the central northern Jan Mayen Ridge. On the other hand, the profile has yielded the crustal velocity distribution to greater depths than previously known. Comparison of the ESP-5 results with velocity-depth relationships in various other geological provinces documents:

- a first-order similarity with data from thinned subsided crust at the Norwegian margin.
- significant differences compared with results from profiles in transitional crust and in Icelandic type of oceanic crust.

By integrating the crustal velocities and layer thickness measured at ESP-5 with available geological information from the ridge complex and with data from areas that were adjacent to the ridge prior to the early Cenozoic opening of the Norwegian-Greenland Sea, we believe that the ESP-5 results are most compatible with the ridge being underlain by a thinned fragment of continental crust.

Acknowledgements. – Data acquisition and processing were funded through the National Science Foundation under grants DPP78-05733 and DP80-19461 and through contributions by participating members of the Lamont-Doherty Geological Observatory's Industrial Associates. We wish to thank Eirik Sundvor and Kristen Haugland for organizing the Norwegian field operations and John C. Mutter and Joyce Alsop for assistance during the data processing. Most of the work was carried out when the senior author was visiting the Lamont-Doherty Geological Observatory supported by the Norwegian Research Council for Science and the Humanities. The project has also, in part, been supported by Statoil and the Norwegian Petroleum Directorate.

References

Carlson, R. L., Christensen, N. I. & Moore, R. P. 1980: Anomalous crustal structure in ocean basin: Continental fragments and oceanic plateaus. *Earth Planet. Sci. Lett. 51*, 171–180.

Diebold, J. B. & Stoffa, P. L. 1981: The traveltime equation, tau-p mapping and inversion of common midpoint data. *Geophysics 46*, 238–254.

Eggen, S. S. 1984: Jan Mayen-ryggens geologi. *NPD-Contribution 20.* 29 pp.

Eldholm, O. & Mutter, J. C. 1986: Basin structure on the Norwegian margin from analysis of digitally recorded sonobuoys. *J. Geophys. Res. 91*, 3763–3783.

Eldholm, O., Thiede, J., Taylor, E. et al. 1987: *Proceedings of the Ocean Drilling Program, Initial Rept. 104 (Pt. A).* 783 pp.

Forsyth, D. A. & Mair, J. A. 1984: Crustal structure of the Lomonosov Ridge and the Fram and Makarov basins near the North Pole. *J. Geophys. Res. 89*, 473–481.

Gairaud, H., Jacquart, G., Aubertin, F. & Beuzart, P. 1978: The Jan Mayen Ridge. Synthesis of geological knowledge and new data. *Oceanologica Acta 1*, 335–358.

Grønlie, G. & Talwani, M. 1982: The free-air gravity field of the Norwegian-Greenland Sea and adjacent areas. *Earth Evol. Ser. 2*, 79–103.

Gudlaugsson, S. T., Gunnarsson, K., Sand, M. & Skogseid, J. 1988: Tectonic and volcanic events at the Jan Mayen Ridge microcontinent. *J. Geol. Soc. London Spec. Paper* (in press).

Johansen, B. 1988: *Geophysical studies of some key areas from Iceland to Svalbard: Reykjanes Ridge, Jan Mayen Ridge, the Norwegian-Greenland Sea and the Barents Sea.* Dr. scient. thesis, Univ. Oslo (in press).

Mutter, J. C., Talwani, M. & Stoffa, P. L. 1984: Evidence for a thick oceanic crust adjacent to the Norwegian margin. *J. Geophys. Res. 89*, 483–502.

Myhre, A. M. 1984: Compilation of seismic velocity measurements along the margins of the Norwegian-Greenland Sea. *Nor. Polarinst. Skr. 180*, 47–67.

Myhre, A. M., Eldholm, O. & Sundvor, E. 1984: The Jan Mayen Ridge: present status. *Polar Research 2 n.s.*, 47–59.

Nunns, A. G. 1983: Plate tectonic evolution of the Greenland-Scotland Ridge and surrounding regions. Pp. 11–30 in Bott, M. H. P. et al. (eds.): *Structure and Development of the Greenland-Scotland Ridge.* Plenum Press, New York.

Skogseid, J. & Eldholm, O. 1987: Early Cenozoic crust at the Norwegian continental margin and the conjugate Jan Mayen Ridge. *J. Geophys. Res. 92*, 11471–11491.

Stoffa, P. L. & Buhl, P. 1979: Two-ship multichannel seismic experiments for deep crustal studies. *J. Geophys. Res. 84*, 7645–7660.

Stoffa, P. L., Buhl, P., Diebold, J. B. & Wentzel, F. 1981: Direct mapping of seismic data in the domain of intercept time and ray parameter – a plane wave decomposition. *Geophysics 45*, 255–267.

Talwani, M. & Eldholm, O. 1977: Evolution of the Norwegian-Greenland Sea. *Geol. Soc. Am. Bull. 88*, 969–999.

Talwani, W., Udintsev, G. et al. 1976: *Initial reports of the Deep Sea drilling Project 38.* U.S. Government Printing Office, Washington. 1256 pp.

Weigel, W. & Gebhardt, V. 1986: Deep structure of the Jan Mayen Ridge (abstr.). *Terra Cognita 6*, 352.